



OPEN

SUBJECT AREAS:
BIOPHYSICS
BIOPHOTONICSReceived
9 May 2014Accepted
10 October 2014Published
7 November 2014Correspondence and
requests for materials
should be addressed to
S.M. (smohanty@uta.
edu)* These authors
contributed equally to
this work.† Current address:
Department of Physics,
New York University,
NY-10012.

Loop formation and self-fasciculation of cortical axon using photonic guidance at long working distance

Argha Mondal^{1*†}, Bryan Black^{1*}, Young-tae Kim² & Samarendra Mohanty¹¹Biophysics and Physiology Lab, Department of Physics; ²Department of Bioengineering, The University of Texas at Arlington, TX 76019.

The accuracy of axonal pathfinding and the formation of functional neural circuitry are crucial for an organism to process, store, and retrieve information from internal networks as well as from the environment. Aberrations in axonal migration is believed to lead to loop formation and self-fasciculation, which can lead to highly dysfunctional neural circuitry and therefore self-avoidance of axons is proposed to be the regulatory mechanism for control of synaptogenesis. Here, we report the application of a newly developed non-contact optical method using a weakly-focused, near infrared laser beam for highly efficient axonal guidance, and demonstrate the formation of axonal loops in cortical neurons, which demonstrate that cortical neurons can self-fasciculate in contrast to self-avoidance. The ability of light for axonal nano-loop formation opens up new avenues for the construction of complex neural circuitry, and non-invasive guidance of neurons at long working distances for restoration of impaired neural connections and functions.

Our bodies contain nearly one thousand billion neurons and those neurons share trillions of connections between them. These connections are facilitated by the outgrowth of axons, which are required to find their paths and targets among heterogeneous neural tissue both over the short and long range (up to one meter). Such axonal pathfinding is highly dynamic in nature and is the most important factor in successful synaptogenesis¹ and formation of functional neuronal networks, which begins at neurogenesis² and continues into adulthood³. For example, in the tectum, which controls auditory and visual responses, both long and short axonal-bundles take erratic routes, crossing each other and the tectal equator. Self-avoidance^{4–5} is a key mechanism in synaptogenesis regulation, and allows neuronal processes to avoid self-fasciculation and loop formation. Remarkably, some self-avoiding neurons discriminate self from foreign cells and interact freely with other neurons of the same subtype, but not with itself⁶. This is especially important during development^{7–8}, when long-range projections span different regions of the nervous system. Axonal pathfinding within the brain as well as in the peripheral nervous system is also crucial for *in vivo* restoration of function subsequent to damage and regeneration. An inability of axons to find their correct paths leads to abnormalities within circuit formations, and thus leads to nervous system dysfunction. Such defects are believed to be primarily biochemical⁹ or genetic^{10–12} in origin, and are related to birth defects such as autism¹³, tuberous sclerosis complex¹⁴ and retinal dysplasias¹⁵. Furthermore, in chemically-treated retinas, axons have been shown¹⁶ to exhibit highly abnormal courses, including circular routes and hairpin loops. However, it is not known if a normal healthy axon would like to fasciculate over itself under the influence of external physical obstructions or physico-chemical cues. This scenario is highly physiological in many cases such as the narrow physical dimension of the exit point (blind spot) in retinas, where the optic nerve leaves the eye. Since earlier attempts have relied on confinement and guidance of axons by physical¹⁷ channels or chemical cues¹⁸, there has not been the required spatial and/or temporal resolution to allow formation of small loops in single axons. It is therefore unclear if a physical or chemical obstruction to a healthy, normal axon would just turn the axon away from its original path or if it can actually lead to self-fasciculation and loop-formation.

Besides topographical¹⁷ and chemical¹⁸ cues, a wide variety of other innovative methods, including electrical¹⁹, optical^{20–23}, and hybrid approaches such as electro-chemical²⁴, optofluidic flow²⁵ and photo-chemical²⁶ cues have been employed for the purposes of axonal guidance. While existing optical methods are based on attractive-guidance principles, we have found that a near-infrared (NIR) laser beams can act as a repulsive cue^{27–28}. Here, we have utilized a weakly-focused NIR laser beam to guide rat cortical axons in a highly effective manner, which has



allowed us to construct loops of varying radii and observe axonal fasciculation for the first time. With accelerated implementation and integration of this enabling technology with other optical manipulation and imaging tools, we envision an effective means to construct and study the basic building blocks of neuronal circuitry *in vitro* with high fidelity and ultimately to understand and control the complex *in vivo* neural circuitry in both the spatial and temporal domains. Ultimately, this method may also provide new opportunities to treat disorders of the nervous system related to axonal misguidance.

Results and Discussion

Though light has been shown to act as an attractive cue while directly impinging on the growth cone (with specific irradiation schedules), we have utilized an at-a-distance effect using a weakly-focused NIR light source which we currently believe to be photothermal^{28–29}. For loop-formation reported here, axons advancing at a growth rate of $> 20 \mu\text{m/hr}$ were randomly selected. Further, the laser spot is not only applied at a transverse distance (2–8 μm) from the growth cone (GC), but the low NA lens (0.5 NA, 20 \times microscope objective) is at an axial distance of $\sim 3 \text{ mm}$. Nevertheless, this should not be interpreted as representing the maximum depth limit that is likely to be employable for future applications. No special efforts were taken to tightly focus the laser beam at the sample plane. In Fig. 1a, we show the schematic of the optical guidance set up, with cortical neurons placed inside the environmental chamber, providing temperature and CO_2 control. Fig. 1b shows an example of laser assisted navigation of rat cortical neurons. The left panel in Fig. 1b shows images of a typical axon before and after a single laser spot has been positioned asymmetrically in front of the GC (position marked by red circle). The time-lapse overlay of the axonal shaft during ‘right’ turn (away from the laser spot) is shown in the right panel (Fig. 1b). Suppl. Movie 1 shows an image sequence of a single-stage optical guidance event. Turning angle of $> 20^\circ$ within first 20 minute of interaction with a static laser beam was considered as a successful guidance event. During axonal growth, the filopodia are known to explore the environment and shows dynamic movement (including tilting). Due to the photothermal repulsion, the growth cone of the axon was seen to avoid the laser spot. Though GC is on a 2D surface, it was found that the GC not only turns away from the laser spot, but also gets detached from the surface and has 3D motion (including flipping). Suppl. Movie 2 shows a representative flipping dynamics of a GC (observed with higher temporal resolution) in response to repulsive light-cue. In Suppl. Fig. 2, we show two sets (A & B) of time-lapse sequences of the axonal GC flipping events. The three-dimensional flipping (tilting about X-axis: pitch, and tilting about Y-axis: yaw) of the two-dimensional GC structure has been depicted in different in Suppl. Fig. 2C. It is important to note the relative position of the point of growth cone emergence from the axonal shaft (i.e. apex of the model structure) with respect to the tip of filopodia along with its orientation (pitch and yaw). In order to describe the dynamics of this flipping process, the value of θ and ϕ with respect to the apex (as origin) was estimated by measuring the projection of the GC shape onto the observation (XY) plane as detailed in the methods section. The inset of Suppl. Fig. 2D shows the nomenclature for orientation (flipping and turning) of GC. Suppl. Fig. 2D shows the short-term kinetics (ϕ vs t) of this dynamic flipping process of the GC during interaction with light-induced repulsive cue. In rare incidences, the GC was found to flip more than 90° . The GC turning kinetics (θ vs t) showed that the GC is highly dynamic and the short-term turning process during interaction with the light-induced repulsive cue is oscillatory in nature (Suppl. Fig. 2E). In both the trials, the maximum theta (refer inset in Suppl. Fig. 2D) occurred at the same time interval, i.e. same oscillation period.

While the effectiveness of our optical guidance method at the currently reported parameters has been 100% for turning events ($n = 14$), we wanted to see whether or not multi-staged guidance events

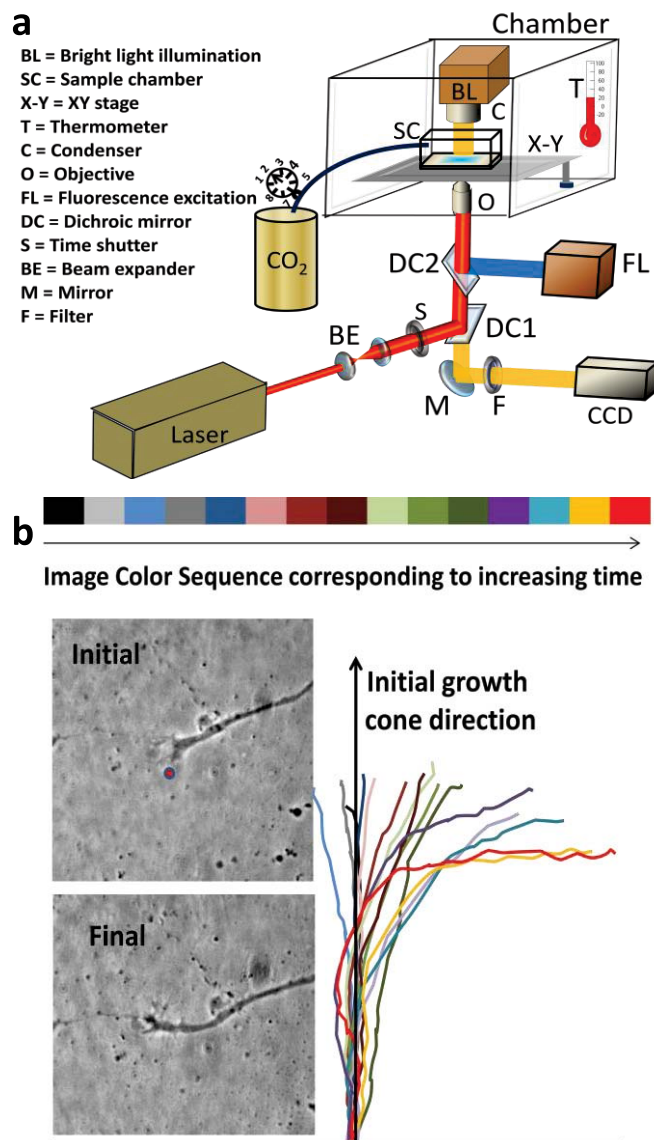


Figure 1 | Laser assisted navigation of rat cortical neurons. (a) Optical guidance set up with environmental chamber. (b) Left panel: image of a typical axon before and after the turn. Laser spot position is marked by red circle. Right panel: time-lapse overlay of axonal shaft turning right after interacting with the laser beam. Initial growth cone direction shown by arrow. Pseudo-color lines drawn over the axonal shaft at different time points and overlaid. In the color bar, the time-interval between colors is 2 min.

could repeatedly turn the GC (by dynamically repositioning the repulsive laser-cue ahead of the advancing GC) and construct an axonal loop. However, in order to avoid spurious results, we first examined whether or not such loops are randomly formed in a normal physiological *in vitro* environment from healthy neurons extracted from the cortical regions of wild-type rats. Though, to date, only genetic and biochemical alterations have been thought to result in aberrant axonal guidance and loop formation, to our surprise, we found random rat cortical neuron loop-formations in the culture platform, albeit at rare incidences (6 out of ~ 400 axonal terminals inspected in 50 random fields of views). Such loops were found to have a radius of curvature ranging from 6 to 22 μm (Suppl. Fig. 1). This observation led us to conclude that without any physical obstruction, a small, but non-negligible percentage (1.5%) of axons may form such loops in normal *in vitro* conditions if they are unable to find a suitable connection site within 2–9 days. This activity may



not necessarily imply an aberrant process, as it could be an effective way by which neurons regulate undesirable synapse formation and optimize their connectivity. However, in order to ascertain that a loop can be formed at any selected point in space and time, we selected random advancing axons (Fig. 2a). Fig. 2b (region of interest marked by rectangle) shows an optically-guided O-loop, which was fabricated from a primary rat cortical neuron. In Fig. 2 (c to k), we show time-lapse zoomed images demonstrating construction of the optically-fabricated axonal loop by a dynamically-repositioned laser spot (marked by red circle, 60 mW, 785 nm).

Formation of the loop (Fig. 2k) demonstrates the unprecedented ability of this repulsive optical cue method to achieve full-circle guidance without any topographical boundaries, which should enable *in situ* formation of complex neuronal circuitry. Interestingly, the radius of curvature of the loop formed by this method can be seen to be $\sim 5 \mu\text{m}$ (equal to the smallest found radius in random loops spontaneously formed *in-vitro*, Suppl. Fig. 1). After optically-guided loop formation (Fig. 2k), though we hypothesized that the GC would advance across the original axonal shaft, the optically-guided rat cortical axon continued to grow along itself, with

self-fasciculation observed over long distances and time (Fig. 2l–n). This leads us to believe that the self-avoidance hypothesis may not be universal for all types of axons and specific neurons may use it to their advantage for forming fascicles with themselves, thus down-regulating synaptogenesis¹⁶. Suppl. Movies 3 & 4 show the zoomed region and full field of view of the O-loop fabrication and self-fasciculation process by spatio-temporal modulation of the laser-induced repulsive cue, respectively. The pseudo-color overlay images of axonal shaft outlines taken from the process of loop formation are shown in Suppl. Fig. 3.

In order to evaluate if the turning angle kinetics are modulated by repeated guidance events, we carried out analysis of turning rates for seven consecutive guidance events. Fig. 3a shows turning angle kinetics of laser-guided rat cortical axon achieved consecutively using a weakly-focused laser beam by a $20\times$ microscope objective. No unidirectional trend between turning rate and sequence number was observed implying that the axon did not lose its ability to turn in response to the repeated repulsive light-cue. Though, for the example shown in Fig. 3a, it appears that the last trial led to the highest turning rate, it is rather random and not the case for all trials. A cumulative

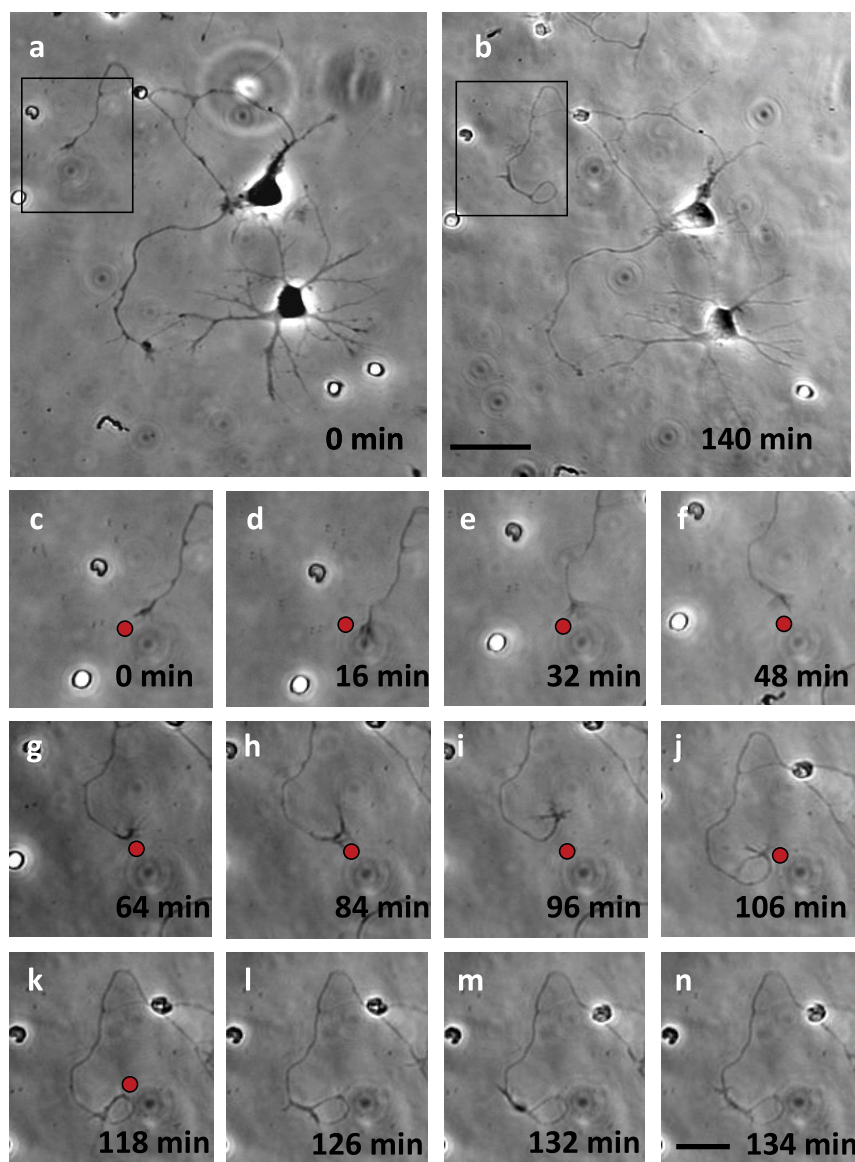


Figure 2 | Laser assisted loop-fabrication and fasciculation of rat cortical neurons. (a) Phase-contrast images of two rat cortical neurons (a) before and (b) after optical guidance. Rectangle showing the region of interest for optical guidance. Scale bar: $50 \mu\text{m}$. (c–k) Time-lapse images of optically-fabricated axonal loop, showing laser spot positions (red circles). (l–n) Self-fasciculation of the axon. Scale bar: $10 \mu\text{m}$.

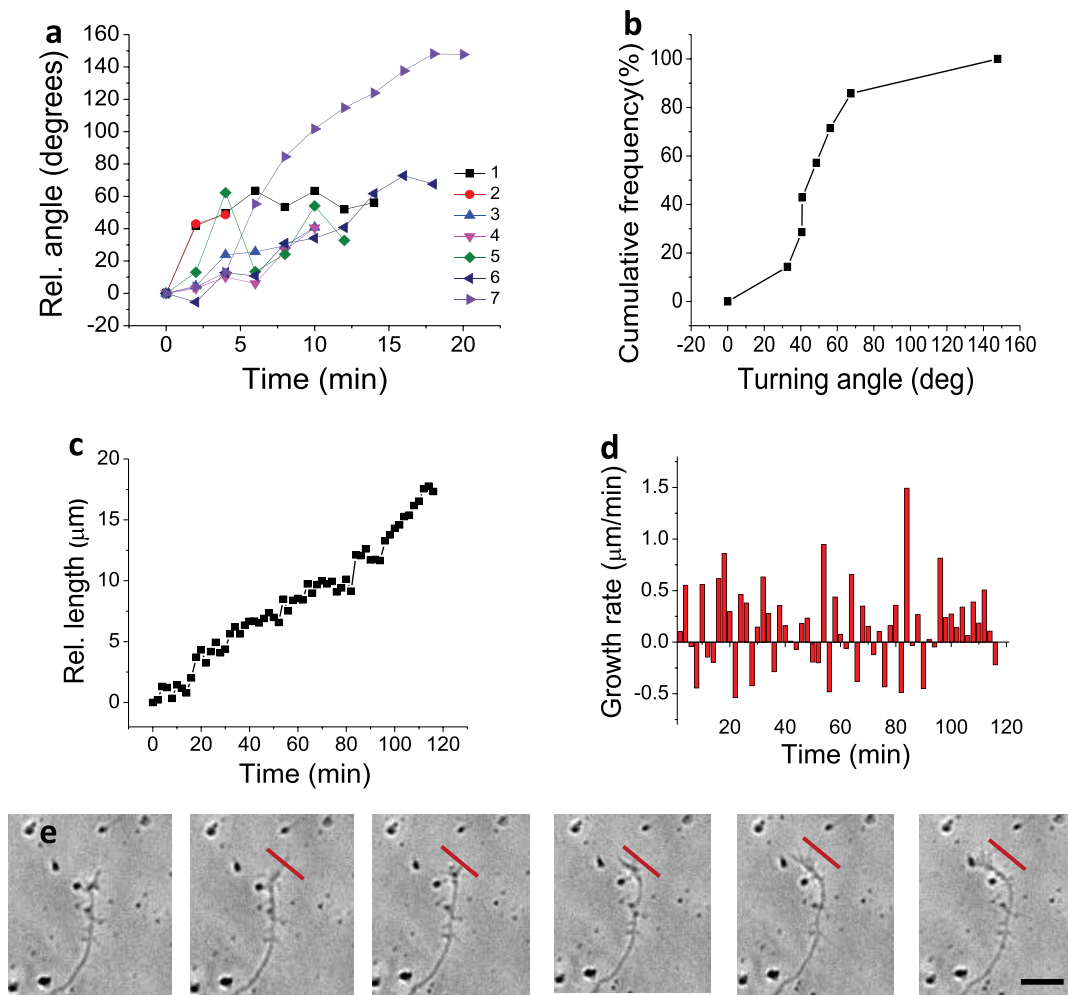


Figure 3 | Kinetics of turning angle and growth during application of spatio-temporally modulated laser guidance. (a) Turning angle kinetics of laser-guided rat cortical axon using 20× microscope objective. (b) Cumulative plots for the distribution of laser-guided axonal turning angles. (c) Kinetics of net axonal growth during optical guidance. (d) Growth rate during multi-stage turning by spatio-temporally modulated laser beam. (e) Time-lapse (3 min) images of axonal guidance using spatially-sculpted line beam profile (marked as red line). Scale bar: 10 μm.

plot for the distribution of laser-guided axonal turning angles is shown in Fig. 3b. It may be noted that in case of axonal stretching, the formation of small bends in an axonal shaft leads to degeneration. For determining the effect of multiple guidance events (during loop formation) on health of axon, net axonal growth as a function of time during optical guidance is measured and shown in Fig. 3c. The growth rate (slope of Fig. 3c) during the (2 hr) multi-stage turning by spatio-temporally modulated laser beam is found to be linear. Remarkably, formation of small axonal loops did not hinder the GC in its growth, as one would have expected due to strain on the intra-cellular microtubule bundles. The instantaneous growth rate (Fig. 3d) depicts the dynamic nature of the small-time scale fluctuations in the axonal growth rate, which is expected due to axons' well-documented stochastic growth behavior. In order to evaluate if spatially-sculpted laser beams can be used to guide axons via repulsive-cue over a relatively large distance, a line profile (10 μm) was created by use of a cylindrical lens in the laser beam (200 mW) path. Fig. 3e shows the time-lapse (3 min) images of axonal guidance using the line spot (marked as red line). The axon was found to migrate with the same avoidance mechanism (Suppl. Movie 5) as shown for circularly-symmetric spot irradiation (Fig. 1 & 2).

Next, we examined if axonal-loops can be formed with smaller radii of curvature using the repulsive-light cue and if self-fasciculation of cortical axon is modulated by such sharp turning processes. In Fig. 4A, we show time-lapse images (a–j) of laser-assisted fabrication

of an axonal loop having radius of curvature < 0.5 μm (measurement limited by resolution of the 20× microscope objective). Suppl. Movie 6 shows the process of l-loop fabrication in optically-guided rat cortical axon using spatio-temporally varying laser spots. The I-loop case seems to resemble with the transient (type-II) GC collapse case³⁰, where the axon did not retract in its length. Though the self-fasciculated axon did not advance at a rate as before, such an I-loop constructed by laser based, repulsive-guidance method raises fundamental physical questions. Namely, what is the smallest radius of curvature that the axon can be bent without irreparably damaging it? The laser assisted repulsive guidance cue could be used to fabricate loops of different radius of curvature intermediary to that shown in Fig. 2 (~5 μm) and Fig. 4A (< 1 μm). Fig. 4B (a–d) shows time-lapse (4 min) phase-contrast images of an e-loop under construction. This loop being elliptic has two radii of curvatures (minor: ~4 μm). In this case also, self-fasciculation of the optically-guided axon was observed (Fig. 4B, e–h). Upon switching off the laser beam, the already-fasciculated axon advanced oppositely along the original axonal shaft (as in Fig. 2). However, in this case, the radius of curvature of the optically-fabricated loop decreased (unlike Fig. 2) to ~1.25 μm as shown in Fig. 4b (e–h). Suppl. Movie 7 shows the process of e-loop fabrication in optically-guided rat cortical axon. Fig. 4C shows kinetics of change in loop diameter as function of time for the different cases (radii) of loop (Fig. 2 vs Fig. 4 A & B). While the larger axonal loop (radius > 5 μm) was found to be stable, stability of

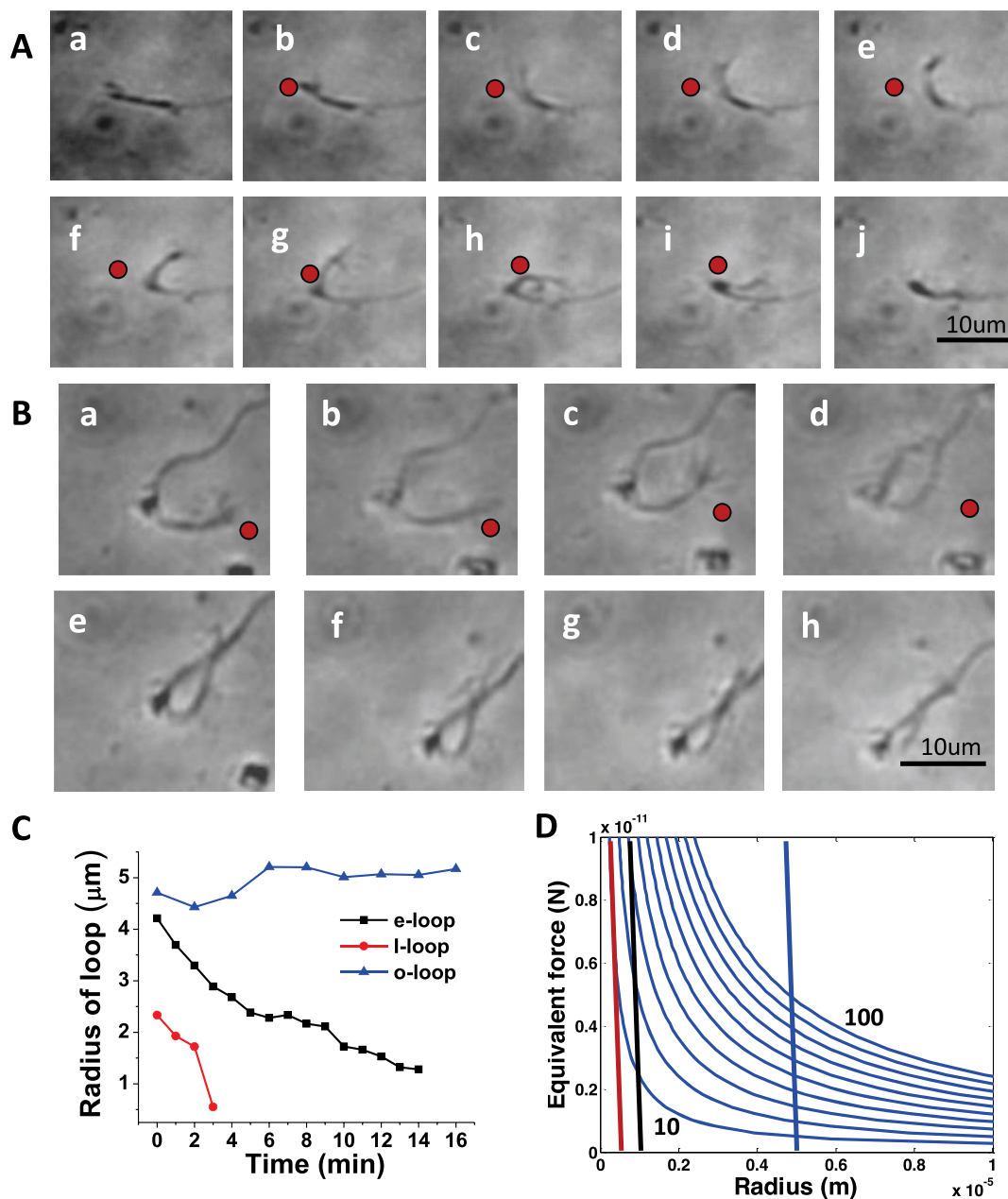


Figure 4 | Laser assisted fabrication of loops of varying radius of curvature in rat cortical neurons. (A) Construction of an I-loop by laser based axonal-guidance method. (a–j) Time-lapse (3 min) phase-contrast images of optically-fabricated I-loop by completely folding a cortical axon back on to its shaft. Scale bar: 10 μm . (B) Laser assisted fabrication of an e-loop. (a–d) Time-lapse (4 min) phase-contrast images of optical fabrication of loop in a rat cortical neuron. (e–h) Self-fasciculation of optically-guided axon and decrease in radius of curvature of the optically-fabricated loop. Scale bar: 10 μm . The positions of laser spot are marked by red circles. (C) Kinetics of change in loop diameter for axonal loops of different radii. (D) Plot of the radius vs equivalent force for axons with different number of microtubules (10–100 in steps of 10). Vertical lines (red: I-loop, black: e-loop, blue: o-loop) indicate three achieved final radii of curvatures of axonal-loops.

smaller loops were found to decrease as the loop radius decreased (Fig. 4C).

To get some insight to the question of minimum possible bending radius that can be achieved in an advancing axon, we modeled the axon as a bundle of microtubules (neglecting the contribution of the axolemma and axoplasm to the mechanical property). Flexural rigidity of single microtubule has been precisely measured earlier by use of optical tweezers³¹. There is a negligible probability that the optical force due to focused laser through 20 \times objective (NA = 0.5) assisted GCs to turn or bend. Our simulations (Lumerical FDTD Solutions 8.6) show that the optical force of a laser beam (focused using a 20 \times microscope objective, NA = 0.5) on a filopodium at a distance of

4 μm is < 0.6 pN/W (Suppl. Fig. 4), whereas typical optical tweezers (realized by 100 \times microscope objective, NA = 1.3) apply forces in the order of 10 pN/W. This implies a force of < 50 fN for 80 mW of laser power used in our guidance experiments with 20 \times microscope objective. Now, we estimated the chemically-transduced (originated from the photothermal-gradient) equivalent-force required to bend an axon (microtubule bundle) to different radii of curvature using the formula detailed in methods. Fig. 4D shows variation of the required equivalent-force as a function of radius with lines denoting the achieved radii of curvatures of axonal-loops. Though the repulsive-optical cue is not photomechanical (optical tweezers) in nature, the strength of this repulsive-cue can be quantified in terms of an equi-



valent force of $\sim 1\text{--}10$ pN (for an axon with 10 microtubules) as determined from Fig. 4D. The equivalent-force required for thicker axons (with more number of microtubules) is found to be higher to cause a similar bending radius in thin axons. Though theoretically (Fig. 4D) it is deemed almost impossible to bend a bundle of let's say 50 microtubules below a radius of curvature of $2\ \mu\text{m}$, experimentally we demonstrated that it is possible to do so. This can be attributed to the fact that in growing axons, the tyrosinated tubulin-rich domain assembles locally near the GC by elongating from the plus end of the stable domain, making it highly dynamic^{32–33}. Our achieved low-bending radius results indicate that the polymerizing labile-domain of the microtubule in GC has very low flexural rigidity as compared to the proximal stable polymer. However, it may be noted that though such small axonal loops have not been naturally observed, microtubule loops with very small radius of curvature is known to occur during synapse formation³⁴. Suppl. Fig. 5 shows the theoretically predicted bending of axon under application of a force of 10 pN for different number of microtubules (10, 40, 70 and 100). To examine if such an indirect repulsive cue is effective in inhibiting loop-formation, we positioned the laser beam in front of the GC (nearer to axon) of already-bending axon (forming a loop).

After we demonstrated that it is possible to facilitate loop formation with small radii of curvature, we aimed to examine the possibility of preventing prospective naturally-occurring loop-formation *in vitro*. We prefer to say prospectively because it is not absolutely certain if the axons selected for loop prevention were going to form loops. However, the selected axons' trajectories prior to application of the optical guidance cue put them on direct course for loop formation. Fig. 5A shows an advancing axon (0 min), which is observed to be on course for loop formation. The application of the NIR optical guidance cue (location marked by red circle) resulted in repulsive guidance (upwards turn, 7 min). After advancing beyond the static position of the laser spot, the axon again made a downward turn (12 min) towards itself and the laser spot was repositioned again into the axon's path. The axon again turned upward and continued to advance at near constant rate (Fig. 5A, 15 min). The laser was not repositioned further to see whether the axon would continue to turn towards itself. Indeed it did, and eventually formed a complete loop and was observed to fasciculate along itself at a still-constant rate (Fig. 5B). Complete dynamics of the relative angle turned and relative length as a function of time are shown in Fig. 5B & C respectively. Although this is a single trial, it implies two things: that the axon may be programmed (at some point in its lifetime) to form a loop and engage in self-fasciculation, regardless of the presence of transient cues which direct it away from itself. The results also imply that the transduced-force provided by the optical guidance cue is greater than whatever force is causing the axon to engage in loop formation (whether it is programmed or not). Further single-stage axon loop prevention trials were also conducted, and resulted in prospective loop prevention three out of four times (Suppl. Fig. 6 A and B).

Evidently, the non-contact repulsive-optical guidance cue approach can be suitably employed for construction of desired neural circuit based on single neuron in 1-dimension (e.g. autopsy³⁵) to many neurons (1 dimension and 2 dimensions) on planar substrate allowing electronic or optical probing (stimulation as well as recording) of the basic neuronal circuitry from the computational^{36–38} as well as device³⁹ point of view. For achieving high throughput construction of neuronal network, a spatio-temporally modulated laser beam could be applied. With ongoing developments in digital light projectors (DLPs) and spatial light modulators (SLMs), laser beams can now be interactively scanned or sculpted to form a laser-repulsive net for organizing the neuronal processes. Construction of *in vitro* neuronal circuitry with high fidelity will allow us to probe and understand the functions of complex neuronal networks *in vivo*. A laser microbeam could be used as optical tweezers, for positioning the neuron and/or guiding the axon, as well as optically monitoring

the neuron's activity^{40–41}. Furthermore, different topological neuronal circuits in three-dimensions can be achieved by first positioning the cells in a 3D array using holographic optical tweezers⁴² and then guiding the axons to desired cell by the optical method described here. Further, the use of ultrafast near-infrared laser scissors^{23,43} would allow nano-surgical elimination of undesired connections in the neuronal network architecture. Such capabilities will allow several key outstanding questions in neuroscience to be answered, including those concerning paths of information flow, details of computation that occurs in a neuronal circuit, how such information processing develops, transferred to different network-elements, and recovered during regeneration after injury^{44,45}.

With the recent advances in the fields of novel optical stimulation and imaging tools⁴⁰, all-optical testing of the computational nature of the optically-fabricated neuronal circuit could be done non-invasively. Furthermore, with the near-infrared laser finding uses in sensitizing neurons by transfection of opsin-encoding genes⁴⁶, and also for two-photon optogenetic stimulation⁴⁰ and optical imaging^{40–41}, rapid progress can be made in the all-optical control of neuronal circuit formation and activity. While this repulsive-guidance cue has been found to be ubiquitous for different types of neurons (Goldfish retinal ganglion cells, rat cortical neuron and dorsal root ganglion cells), with integration of bio and conformable nanophotonics technologies⁴⁷, new possibilities will emerge to genetically sensitize specific neurons to respond to specific laser wavelengths and thus guide them selectively *in vivo*.

Conclusions

Our non-contact approach demonstrates the remarkable capability of non-invasively navigating axons with very high efficiency and high spatio-temporal resolution at large working distances. This is demonstrated by the formation of loops with varying radii. While self-fasciculation was found to be preferred in rat cortical neurons, in disagreement with the self-avoidance hypothesis, it may not be ubiquitous to all neuronal types. Furthermore, it is undeniable that, since there is a non-zero probability of finding naturally occurring loops *in vitro*, we cannot say that the loops formed during multi-staged guidance trials were not going to form naturally, without the application of the NIR optical guidance cue. What we can say is that it is incredibly unlikely that loop formation would have occurred in the direction opposite to the arbitrary asymmetrical placement of the optical cue, and that the loops we observed during guidance trials resulted in loop radii which were significantly smaller than those of loops found naturally occurring *in vitro*. At the very least, we can confidently claim that the repulsive optical guidance cue facilitates cortical axon loop formation *in vitro* and could prove invaluable in the future study of aberrant, as well as typical, neuronal circuitry formation. The ability of spatio-temporally modulated light for enabling axonal nano-loop formations opens up new vistas in the physical and biological analysis of neuronal circuitry processes. With a bottom-up approach, we believe our method could enable construction of a three-dimensional neuronal structure in the future, which will help us to understand the neuronal activity of the brain.

Methods

The experimental procedures reported in this manuscript were conducted according to The University of Texas at Arlington's Institutional Animal Care and Use Committee approved protocol.

Cortical neuron culture. All experimental procedures were conducted according to Institutional Animal Care and Use Committee approved protocol. The cortical neurons were isolated from embryonic 18 day rat embryos. The cortical tissues were dissected, cleaned (meningeal layer), enzymatically dissociated (0.125% trypsin in L-15 medium) for 20 minutes at 37°C . The dissociated cortical neurons (100,000/device) were seeded on Poly-D-lysine (PDL, 0.01%, Sigma) pre-coated coverglass with Polydimethylsiloxane barrier (Sylgard 184, Dow corning), and the serum-free culture medium (Neurobasal medium supplemented B-27 with BDNF and NT-3, 10 ng/ml) was changed every 3 days.

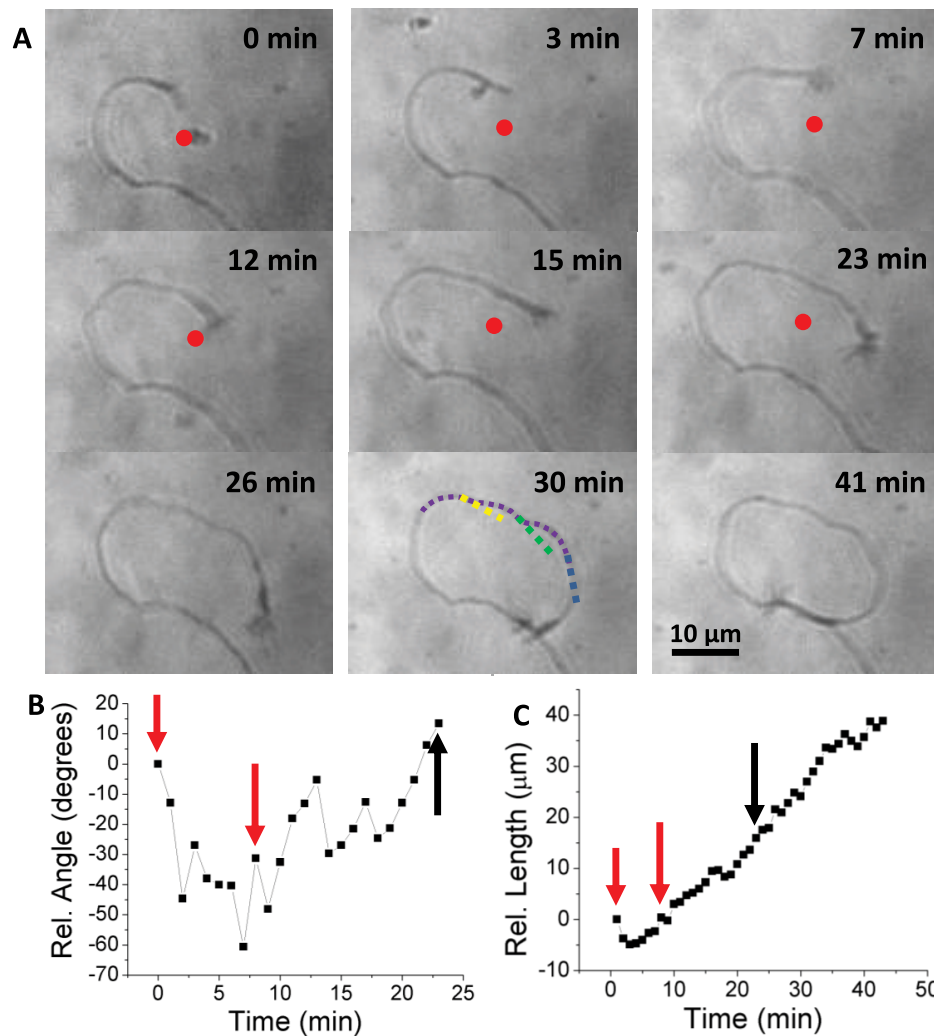


Figure 5 | Laser-assisted axonal loop prevention. (A) Time-lapse series of phase contrast images demonstrating prevention of prospective loop formation by repulsive optical cue in the case of rat cortical axons (laser spot marked by red circle). Laser spot was repositioned after 8 minutes and turned off after 23 minutes. Axon is observed to fasciculate on itself for duration of observation following 26 minutes. (B) Dynamics of relative angle turned during loop prevention due to initial (short red arrow) and secondary (long red arrow) optical guidance. (C) Dynamics of relative length during loop prevention due to initial (short red arrow) and secondary (long red arrow) optical guidance. The termination of optical guidance is denoted by a black arrow.

Set up for axonal navigation. The schematic of the platform for axonal navigation is shown in Fig. 1a. A tunable near-infrared Ti: Sapphire laser (MaiTai HP, Newport-SpectraPhysics) beam, operated in mode-lock off condition was expanded and relayed via folding mirrors to the back-laser port of an inverted microscope (Ti-U Eclipse, Nikon). A mechanical shutter (Uniblitz) was used to pulse the laser beam (20 ms ON and 20 ms OFF) in order to avoid continuous temperature rise or mechanical forcing. A dichroic mirror was used to guide the beam to the back-aperture of a 20× microscope objective (Ph1, NA = 0.5, Nikon), while transmitting the visible light for phase contrast imaging. An IR cut-off filter was used in the imaging path for removing the reflected laser beam to reach the CCD (Photometrics). The wavelength and power of the laser beam was adjusted via software so as to result in a sample-site beam power of ~80 mW. The laser power at the sample plane was calculated by multiplying the transmission factor of the objective with the power measured at the back aperture of the microscope objective using a standard light power meter (PM 100D, Thorlabs). To achieve optical guidance, the beam was placed beyond the axons' filopodia, asymmetrically positioned in the path of the growing axons.

Measurement of orientation of growth cone. The initial axonal orientation is marked as reference and the subsequent turnings were measured with respect to that initial position. Due to the action of force on the growth cone the growth cone also avoids the laser spot. In order to do so it has been observed that the GC not only turns away from the laser spot, it also flips back. This flipping dynamics has been quantified by noting the change in projection of the growth cone on the flat surface using Image J software. Whenever the GC lifts up from the surface, we only see the projected lengths in X and Y-directions. By taking the ratio of original GC length to lifted GC projection length we can easily obtain the flip angle.

Theoretical calculation of equivalent force required to cause observed axonal bending radius. Microtubules are long filaments, which serve as tracks for intercellular motor proteins and facilitate the structural functions in eukaryotic cells. In a typical axon, 10 to 100 such microtubules are assumed⁴⁸ to be present in any given axonal shaft cross-section. The axonal growth cone polymerization processes are modulated asymmetrically by the photothermal-gradient generated by the near-infrared laser beam which results in a chemically-transduced 'equivalent force'. To analyze the deformation, or bending, of an axon due to force on its tip (growth cone), we modeled the axon as a beam of regular and uniform cross-section, made of a linear elastic material (microtubule with known⁴⁸ flexural rigidity) that is homogeneous and isotropic with the load concentrated at the axonal terminal. The methodologies used to quantify these deflections can basically be categorized into analytical or finite element analysis techniques. The analytical method is based on Euler-Bernoulli's (EB's) theory, which provides a means to quantify such deflections. Then, the finite element method is utilized to obtain the solution of the bending radius of curvature of an axonal shaft under constant force at the tip. Details described in supplementary methods.

1. Kwon, H. B. *et al.* Neuroligin-1-dependent competition regulates cortical synaptogenesis and synapse number. *Nat Neurosci* **15**, 1667–1674 (2012).
2. Singer, M., Nordlander, R. H. & Egar, M. Axonal guidance during embryogenesis and regeneration in the spinal cord of the newt: the blueprint hypothesis of neuronal pathway patterning. *J Comp Neurol* **185**, 1–21 (1979).
3. Hand, R. & Polleux, F. Neurogenin2 regulates the initial axon guidance of cortical pyramidal neurons projecting medially to the corpus callosum. *Neural Dev* **6**, 30–45 (2011).



4. Matthews, B. J. *et al.* Dendrite self-avoidance is controlled by Dscam. *Cell* **129**, 593–604 (2007).
5. Smith, C. J., Watson, J. D., VanHovene, M. K., Colon-Ramos, D. A. & Miller, D. M. Netrin (UNC-6) mediates dendritic self-avoidance. *Nat Neurosci* **15**, 731–737 (2012).
6. Lefebvre, J. L., Kostadinov, D., Chen, W. S. V., Maniatis, T. & Sanes, J. R. Protocadherins mediate dendritic self-avoidance in the mammalian nervous system. *Nature* **488**, 517–521 (2012).
7. Fuerst, P. G., Koizumi, A., Masland, R. H. & Burgess, R. W. Self-avoidance mediated by DSCAM in the developing mammalian retina. *Int J Dev Neurosci* **26**, 832–832 (2008).
8. Jhaveri, S., Erzurumlu, R. S. & Schneider, G. E. The optic tract in embryonic hamsters: Fasciculation, defasciculation, and other rearrangements of retinal axons. *Visual Neurosci* **13**, 359–374 (1996).
9. Huettl, R. E., Haehl, T. & Huber, A. B. Fasciculation and Guidance of Spinal Motor Axons in the Absence of FGFR2 Signaling. *PLoS One* **7**, e41095, 1–10 (2012).
10. Favero, C. B. *et al.* Mutation of the BiP/GRP78 gene causes axon outgrowth and fasciculation defects in the thalamocortical connections of the mammalian forebrain. *Journal of Comparative Neurology* **521**, 677–696 (2013).
11. Baum, P. D. & Garriga, G. Neuronal migrations and axon fasciculation are disrupted in *ina-1* integrin mutants. *Neuron* **19**, 51–62 (1997).
12. Engle, E. C. Human genetic disorders of axon guidance. *Cold Spring Harb Perspect Biol* **2**, a001784 (2010).
13. Minshew, N. J. & Williams, D. L. The new neurobiology of autism: cortex, connectivity, and neuronal organization. *Arch Neurol* **64**, 945–950 (2007).
14. Choi, Y. J. *et al.* Tuberous sclerosis complex proteins control axon formation. *Genes Dev* **22**, 2485–2495 (2008).
15. Weiner, J. A. *et al.* Axon fasciculation defects and retinal dysplasias in mice lacking the immunoglobulin superfamily adhesion molecule BEN/ALCAM/SC1. *Mol Cell Neurosci* **27**, 59–69 (2004).
16. Wahle, P., Meyer, G., Wu, J. Y. & Albus, K. Morphology and axon terminal pattern of glutamate decarboxylase-immunoreactive cell types in the white matter of the cat occipital cortex during early postnatal development. *Brain Res* **433**, 53–61 (1987).
17. Hoffman-Kim, D., Mitchel, J. A. & Bellamkonda, R. V. Topography, Cell Response, and Nerve Regeneration. *Annu Rev Biomed Eng* **12**, 203–231 (2010).
18. Ming, G. L. *et al.* Adaptation in the chemotactic guidance of nerve growth cones. *Nature* **417**, 411–418 (2002).
19. Patel, N. & Poo, M. M. Orientation of Neurite Growth by Extracellular Electric Fields. *J Neurosci* **2**, 483–496 (1982).
20. Ehrlicher, A. *et al.* Guiding neuronal growth with light. *P Natl Acad Sci USA* **99**, 16024–16028 (2002).
21. Mohanty, S. K., Sharma, M., Panicker, M. M. & Gupta, P. K. Controlled induction, enhancement, and guidance of neuronal growth cones by use of line optical tweezers. *Opt Lett* **30**, 2596–2598 (2005).
22. Mathew, M. *et al.* Signalling effect of NIR pulsed lasers on axonal growth. *J Neurosci Meth* **186**, 196–201 (2010).
23. Wu, T. *et al.* Neuronal growth cones respond to laser-induced axonal damage. *Journal of The Royal Society Interface* **9**, 535–547 (2012).
24. Blau, A. *et al.* Promotion of neural cell adhesion by electrochemically generated and functionalized polymer films. *J Neurosci Meth* **112**, 65–73 (2001).
25. Wu, T. *et al.* A photon-driven micromotor can direct nerve fibre growth. *Nature Photonics* **6**, 62–67 (2012).
26. Luo, Y. & Shoichet, M. S. A photolabile hydrogel for guided three-dimensional cell growth and migration. *Nat Mater* **3**, 249–253 (2004).
27. Black, B., Mondal, A., Kim, Y. & Mohanty, S. K. Neuronal beacon. *Opt Lett* **38**, 2174–2176 (2013).
28. Black, B. J., Gu, L. & Mohanty, S. K. Highly effective photonic cue for repulsive axonal guidance. *PLoS One* **9**, e86292 (2014).
29. Black, B., Mondal, A., Kim, Y. & Mohanty, S. K. Neuronal beacon. *Opt Lett* **38**, 2174–2176 (2013).
30. Rauch, P., Heine, P., Goettgens, B. & Kas, J. A. Different modes of growth cone collapse in NG 108-15 cells. *Eur Biophys J* **42**, 591–605 (2013).
31. Felgner, H., Frank, R. & Schliwa, M. Flexural rigidity of microtubules measured with the use of optical tweezers. *J Cell Sci* **109**, 509–516 (1996).
32. Ahmad, F. J., Pienkowski, T. P. & Baas, P. W. Regional differences in microtubule dynamics in the axon. *J Neurosci* **13**, 856–866 (1993).
33. Conde, C. & Caceres, A. Microtubule assembly, organization and dynamics in axons and dendrites. *Nat Rev Neurosci* **10**, 319–332 (2009).
34. Roos, J., Hummel, T., Ng, N., Klambt, C. & Davis, G. W. Drosophila Futsch regulates synaptic microtubule organization and is necessary for synaptic growth. *Neuron* **26**, 371–382 (2000).
35. Seung, H. S., Lee, D. D., Reis, B. Y. & Tank, D. W. The autapse: a simple illustration of short-term analog memory storage by tuned synaptic feedback. *J Comput Neurosci* **9**, 171–185 (2000).
36. Koch, C. Computation and the single neuron. *Nature* **385**, 207–210 (1997).
37. Gabbiani, F., Krapp, H. G., Koch, C. & Laurent, G. Multiplicative computation in a visual neuron sensitive to looming. *Nature* **420**, 320–324 (2002).
38. Hatsopoulos, N., Gabbiani, F. & Laurent, G. Elementary Computation of Object Approach by a Wide-Field Visual Neuron. *Science* **270**, 1000–1003 (1995).
39. DeMarse, T. B. & Dockendorf, K. P. Adaptive flight control with living neuronal networks on microelectrode arrays. *Proc. IJCNN*, 1–5, 1548–1551 (2005).
40. Mohanty, S. K. *et al.* In-depth activation of channelrhodopsin 2-sensitized excitable cells with high spatial resolution using two-photon excitation with a near-infrared laser microbeam. *Biophys J* **95**, 3916–3926 (2008).
41. Choudhury, N., Zhang, Z., Zhao, F., Gu, L. & Mohanty, S. Label-free optical detection of optogenetic activation of cells using phase-sensitive Fourier domain optical coherence tomography. *Visualiz Image Proc Computat Biomed* **1**, 2012004984 (2012).
42. Curtis, J. E., Koss, B. A. & Grier, D. G. Dynamic holographic optical tweezers. *Opt Commun* **207**, 169–175 (2002).
43. Kim, Y. T., Karthikeyan, K., Chirvi, S. & Dave, D. P. Neuro-optical microfluidic platform to study injury and regeneration of single axons. *Lab Chip* **9**, 2576–2581 (2009).
44. McDonald, J. W., Gottlieb, D. I. & Choi, D. W. What is a functional recovery after spinal cord injury? *Nat Med* **6**, 358–358 (2000).
45. Hellal, F. *et al.* Microtubule stabilization reduces scarring and causes axon regeneration after spinal cord injury. *Science* **331**, 928–931 (2011).
46. Gu, L. & Mohanty, S. K. Targeted microinjection into cells and retina using optoporation. *J Biomed Opt* **16**, 128003, 1–6 (2011).
47. Yang, H. J. *et al.* Transfer-printed stacked nanomembrane lasers on silicon. *Nat Photonics* **6**, 615–620 (2012).
48. Peter, S. J. & Mofrad, M. R. Computational modeling of axonal microtubule bundles under tension. *Biophys J* **102**, 749–757 (2012).

Acknowledgments

SM would like to thank the support from Office of President and Provost, The University of Texas at Arlington and the National Science Foundation (1148541) and National Institute of Health (NS084311).

Author contributions

A.M., B.B. and S.M. performed the experiments and analyzed the data. A.M. modeled the axonal bending; Y.K. performed cortical neuron culture, developed the culture chamber and participated in discussion. S.M. designed and supervised the project. All authors wrote the paper.

Additional information

Supplementary information accompanies this paper at <http://www.nature.com/scientificreports>

Competing financial interests: The authors declare no competing financial interests.

How to cite this article: Mondal, A., Black, B., Kim, Y.-t. & Mohanty, S. Loop formation and self-fasciculation of cortical axon using photonic guidance at long working distance. *Sci. Rep.* **4**, 6902; DOI:10.1038/srep06902 (2014).



This work is licensed under a Creative Commons Attribution-NonCommercial-ShareAlike 4.0 International License. The images or other third party material in this article are included in the article's Creative Commons license, unless indicated otherwise in the credit line; if the material is not included under the Creative Commons license, users will need to obtain permission from the license holder in order to reproduce the material. To view a copy of this license, visit <http://creativecommons.org/licenses/by-nc-sa/4.0/>